

**Aim of the study:** The  $^{57}\text{Co}$  radioisotope has recently been proposed as a hypothetical brachytherapy source due to its high specific activity, appropriate half-life (272 days) and medium energy photons (114.17 keV on average). In this study, Task Group No. 43 dosimetric parameters were calculated and reported for a hypothetical  $^{57}\text{Co}$  source.

**Material and methods:** A hypothetical  $^{57}\text{Co}$  source was simulated in MCNPX, consisting of an active cylinder with 3.5 mm length and 0.6 mm radius encapsulated in a stainless steel capsule. Three photon energies were utilized (136 keV [10.68%], 122 keV [85.60%], 14 keV [9.16%]) for the  $^{57}\text{Co}$  source. Air kerma strength, dose rate constant, radial dose function, anisotropy function, and isodose curves for the source were calculated and compared to the corresponding data for a  $^{192}\text{Ir}$  source.

**Results:** The results are presented as tables and figures. Air kerma strength per 1 mCi activity for the  $^{57}\text{Co}$  source was  $0.46 \text{ cGyh}^{-1} \text{ cm}^2 \text{ mCi}^{-1}$ . The dose rate constant for the  $^{57}\text{Co}$  source was determined to be  $1.215 \text{ cGyh}^{-1} \text{ U}^{-1}$ . The radial dose function for the  $^{57}\text{Co}$  source has an increasing trend due to multiple scattering of low energy photons. The anisotropy function for the  $^{57}\text{Co}$  source at various distances from the source is more isotropic than the  $^{192}\text{Ir}$  source.

**Conclusions:** The  $^{57}\text{Co}$  source has advantages over  $^{192}\text{Ir}$  due to its lower energy photons, longer half-life, higher dose rate constant and more isotropic anisotropic function. However, the  $^{192}\text{Ir}$  source has a higher initial air kerma strength and more uniform radial dose function. These properties make  $^{57}\text{Co}$  a suitable source for use in brachytherapy applications.

**Key words:** hypothetical source,  $^{57}\text{Co}$ ,  $^{192}\text{Ir}$ , TG-43 dosimetric parameters, Monte Carlo simulation.

Contemp Oncol (Pozn) 2016; 20 (4):  
327–334  
DOI: 10.5114/wo.2016.61854

# Comparison of the hypothetical $^{57}\text{Co}$ brachytherapy source with the $^{192}\text{Ir}$ source

Mohammad Taghi Bahreyni Toossi<sup>1</sup>, Mahdi Ghorbani<sup>1</sup>, Atefeh Rostami<sup>1</sup>, Mohsen Khosroabadi<sup>2</sup>, Sara Khademi<sup>3</sup>, Courtney Knaup<sup>4</sup>

<sup>1</sup>Biomedical Engineering and Medical Physics Department, Faculty of Medicine, Shahid Beheshti University of Medical Sciences, Tehran, Iran

<sup>2</sup>Faculty of Medicine, North Khorasan University of Medical Sciences, Bojnurd, Iran

<sup>3</sup>Medical Physics and Medical Engineering Department, Faculty of Medicine, Tehran University of Medical Sciences, Tehran, Iran

<sup>4</sup>Comprehensive Cancer Centers of Nevada, Las Vegas, Nevada, USA

## Introduction

Cancer is the third leading cause of death in developed countries [1]. Three major modalities for the treatment of cancer are surgery, chemotherapy and radiation therapy. Radiation therapy is a method in which ionizing radiation is used to treat or relieve cancer. Almost half of all cancer patients receive radiation therapy during their course of treatment. Radiation therapy is classified into two types: externally delivered radiation therapy (teletherapy) and internally delivered radiation therapy (brachytherapy). From the late 1990s, brachytherapy was widely expanded for treatment of tumours of prostate, breast and cervix [2].

In brachytherapy, a radioactive source (radioisotope) is placed in the vicinity of the tumour or within it during treatment.  $^{192}\text{Ir}$  is one of the radioisotopes that are widely used in high dose rate (HDR) brachytherapy.  $^{192}\text{Ir}$  is both a  $\gamma$  and  $\beta$  emitter. The emitted gamma radiation from  $^{192}\text{Ir}$  has an energy range of 201–884 keV, with an average of 360 keV. The average energy for the  $\beta$  particles from  $^{192}\text{Ir}$  decay is 200 keV. The energy of  $\gamma$  and  $\beta$  particles emitted by the  $^{192}\text{Ir}$  source is relatively high, and therefore it is important to have appropriate protection for radiotherapy staff and enough shielding for the treatment room [3]. Taking into account the relatively high energy of this source and the personnel safety needed, it would be useful to search for other sources with lower energy photons, yet sufficient specific activity.

Nowadays, the  $^{57}\text{Co}$  radioisotope is used as a source for calibration of gamma cameras and the study of leukaemia, related to  $\text{B}_{12}$  vitamin deficiency and its insufficient absorption.  $^{57}\text{Co}$  can be produced by an accelerator through  $^{55}\text{Mn}(\alpha, 2n)^{57}\text{Co}$  nuclear reaction. Based on this reaction  $\alpha$  particles interact with  $^{55}\text{Mn}$  and the products are neutrons and  $^{57}\text{Co}$ . This reaction requires  $\alpha$  irradiation, which is not commonly available. Therefore, the efficiency of this reaction is not appropriate for therapeutic applications. As an alternative, high energy proton beams can be used. The target material can be natural iron or nickel and the following reactions occur:  $^{26}\text{Fe}(p, x)^{57}\text{Co}$  or  $^{58}\text{Ni}(p, x)^{57}\text{Co}$ . Use of  $^{57}\text{Ni}$  can cause the production of a large amount of  $^{56}\text{Co}$  nuclides, which are considered as an impurity having a half-life of 79 days. Use of enriched  $^{58}\text{Ni}$  as the target and appropriate selection of proton energy can prevent production of this impurity. Carter and Laird [4] described methods for construction of a radioactive stent and reviewed the experimental information on the treatment for enhancement of arterial patency rates after placement of the stent. They declared that with one-year follow-up after implantation of a radioactive stent with combination of  $\gamma$ - and  $\beta$ -emitting  $^{55}\text{Co}$ ,  $^{56}\text{Co}$ ,  $^{57}\text{Co}$ ,  $^{52}\text{Mg}$ , and  $^{55}\text{Fe}$  radionuclides, approximately complete inhibition of neointimal proliferation was observed in a rabbit model.

Adequate characteristics of  $^{57}\text{Co}$  would be a motivation for more evaluation of this radioisotope for application as a brachytherapy source.

Simulation of a source and calculation of dosimetric parameters presented by Task Group No. 43 (TG-43) for a source is one of the methods for verification of dosimetric characteristics of a brachytherapy source before its clinical usage. Task Group No. 43 describes a formalism for calculation of dosimetric parameters for brachytherapy sources. The dosimetric parameters include air kerma strength, dose rate constant, radial dose function and anisotropy function. After verification of the calculations of dosimetric parameters of the  $^{57}\text{Co}$  source, it can be evaluated whether they are appropriate in comparison with other available brachytherapy sources, then this source may be used in clinical applications.

Up to now,  $^{169}\text{Yb}$  and  $^{170}\text{Tm}$  radioisotopes, due to their medium energy photons, have been proposed as hypothetical sources for use in brachytherapy, and their dosimetric parameters have been reported. Dosimetric parameters of a hypothetical  $^{170}\text{Tm}$  source were studied by Ballester *et al.* [5]. This radioisotope has high specific activity and a half-life of 128 days. It emits photons with average energy of 66.39 keV.  $^{170}\text{Tm}$  has a low photon yield (6 photons per 100 electrons emitted), which is considered a disadvantage for the source. In their simulations, cylindrical and spherical sources were defined inside steel and platinum capsules, respectively. The bremsstrahlung dose contribution had the same order of magnitude as the dose contribution raised from characteristic x-rays and  $\gamma$  photons, due to high electron yield and energetic  $\beta$  particles. The dose rate constant was reported to be  $1.23 \text{ cGyh}^{-1}\text{U}^{-1}$  for the cylindrical source. The results showed that brachytherapy with  $^{170}\text{Tm}$  needs longer treatment duration in comparison with other sources. On the other hand, this source provides a more uniform dose distribution. Enger *et al.* [6] calculated dosimetric parameters for a hypothetical  $^{170}\text{Tm}$  source by means of the Monte Carlo (MC) method. They evaluated the effect of the capsule material on emitted photons' and electrons' energy spectra. In the study, a cylindrical  $^{170}\text{Tm}$  source was designed with active length of 3.5 mm and diameter of 0.6 mm, the same as the Flexisource  $^{192}\text{Ir}$  source. Furthermore, the radial dose function for various materials (stainless steel, gold and platinum) was calculated. The results showed that gold and platinum capsules not only can absorb the emitted  $\beta$  particles but also attenuate low energy photons. The average photon energy transmitted through the source core and the stainless steel capsule was about 113 keV, whereas the average energy transmitted via the gold and platinum capsules was about 160 keV and 165 keV, respectively. Enger *et al.* [7] presented dosimetric characteristics of a hypothetical  $^{153}\text{Gd}$  source. This source is a photon emitting source with 40–100 keV photons and a half-life of 242 days. They simulated the hypothetical  $^{153}\text{Gd}$  source with 0.84 mm diameter and 10 mm length in a stainless steel encapsulation. The results imply that this source would be adequate as a low dose rate or pulsed dose rate brachytherapy source. The  $\beta$  particles emitted by this source are low energy and are absorbed in the source's capsule. An increasing radial

dose function was observed due to multiple scattering of low energy photons of the source. It was concluded that this source can provide brachytherapy treatments with patient-specific shielding and reduced personnel shielding compared to  $^{192}\text{Ir}$ . In order to predict physical parameters useful in treatment planning and radiation protection, Mason *et al.* [8] studied characteristics of a  $^{169}\text{Yb}$  source by Monte Carlo simulation. This radioisotope emits photons with mean energy of 93 keV, and its half-life is 32 days. The air kerma rate constant and dose rate constant for this radioisotope were reported as  $0.427 \text{ cGycm}^2\text{h}^{-1}\text{MBq}^{-1}$  and  $1.8 \text{ Rcm}^2\text{mCi}^{-1}\text{h}^{-1}$ , respectively. The results showed that  $^{169}\text{Yb}$  provides a more uniform dose distribution relative to  $^{192}\text{Ir}$  and  $^{137}\text{Cs}$  sources. Additionally, due to the short half-life of  $^{169}\text{Yb}$  this source is more adequate for interstitial brachytherapy.

Ninkovic *et al.* [9] calculated the air kerma rate constant for point sources of various radionuclides which are practically used. The radionuclides were 35 radionuclides including  $^{57}\text{Co}$ . The calculations were based on corrections for internal conversion of X and  $\gamma$  rays and the generation of the K and L series X rays from internal conversion and electron capture. Air kerma rate constants were calculated for each discrete energy in the photon spectrum of the radionuclides with yield per decay more than 0.01% and with energy higher than 20 keV. They used the latest energy spectrum and mass energy transfer coefficient data and therefore were able to calculate the most accurate air kerma rate constants for the 35 radionuclides. In a study by Enger *et al.* [3] the radial dose function and anisotropy function for a hypothetical  $^{57}\text{Co}$  source were calculated using the Monte Carlo method, and the results were compared with those of  $^{125}\text{I}$  and  $^{192}\text{Ir}$  sources, which are routinely used in brachytherapy.  $^{125}\text{I}$  and  $^{192}\text{Ir}$  have lower and higher average photon energies relative to  $^{57}\text{Co}$ , respectively. An increase in radial dose function was observed for the hypothetical  $^{57}\text{Co}$  source due to an increase in scattered photons resulting from low energy photons. Furthermore, the  $^{57}\text{Co}$  source can provide a more uniform dose distribution relative to the  $^{192}\text{Ir}$  source. However, anisotropy functions of both sources do not differ significantly.

Although some dosimetric parameters of a hypothetical  $^{57}\text{Co}$  source were reported by Enger *et al.* [3], to the best of our knowledge there is not a comprehensive comparison of the data to a  $^{192}\text{Ir}$  source. In the study by Enger *et al.* [3] radial dose function and anisotropy function data were presented only in the form of plots, and the anisotropy function was only calculated for one distance. The aim of this study is to evaluate the  $^{57}\text{Co}$  radioisotope as a source for use in brachytherapy. For this purpose, dosimetric parameters of a hypothetical  $^{57}\text{Co}$  source are calculated by Monte Carlo method and are compared with those of a corresponding  $^{192}\text{Ir}$  source.

## Material and methods

### Geometry of hypothetical $^{57}\text{Co}$ and Flexisource $^{192}\text{Ir}$ sources

In this study the geometry of a hypothetical  $^{57}\text{Co}$  source was considered similar to that of the Flexisource  $^{192}\text{Ir}$

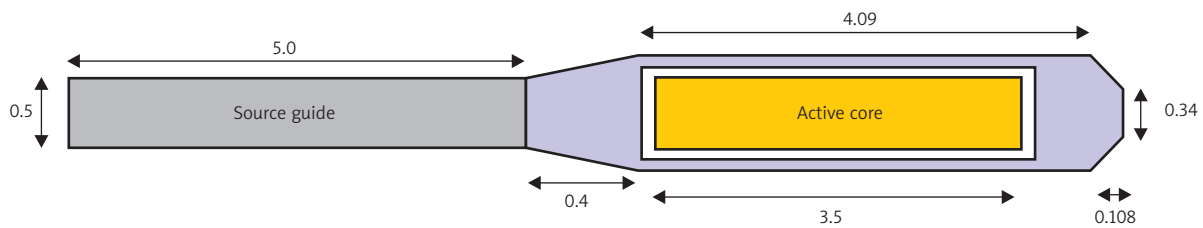


Fig. 1. Geometry of the hypothetical  $^{57}\text{Co}$  source simulated in this study (all dimensions are in millimetres)

source model. In the study by Enger *et al.* [3] on the  $^{57}\text{Co}$  hypothetical source, this geometry was also used. Based on this geometry, the active part of the source was assumed as pure  $^{57}\text{Co}$ , instead of active  $^{192}\text{Ir}$ . The active part was simulated as a cylinder with 3.5 mm length and 0.6 mm diameter located inside a capsule by MCNPX Monte Carlo code (version 2.6.0) [10] (Fig. 1). Herein the density of the  $^{57}\text{Co}$  source was considered the same as  $^{60}\text{Co}$  ( $8.86\text{ g/cm}^3$ ). The source's capsule is made of stainless steel with density of  $8\text{ g/cm}^3$ , and its elemental composition includes: Fe (67.92%), Cr (19%), Ni (10%), Mn (2%), Si (1%) and C (0.08%). The cylindrical part of the source encapsulation has inner and outer radii of 0.335 mm and 0.425 mm, respectively. An air gap with density of  $0.001205\text{ g/cm}^3$  was considered in the space between the active part and the capsule. There are two truncated cones with lengths of 0.108 mm and 0.4 mm at the two ends of the cylindrical part of the capsule. The source cable was modelled as a cylinder with length of 5 mm and radius of 0.25 mm. These parameters which were simulated in this study are based on the studies by Enger *et al.* [3] and Granero *et al.* [11] on a hypothetical  $^{57}\text{Co}$  source and the Flexisource  $^{192}\text{Ir}$  source, respectively.

In the present study, the Flexisource  $^{192}\text{Ir}$  source was also simulated. The geometry of the Flexisource  $^{192}\text{Ir}$  source is similar to that of  $^{57}\text{Co}$  which was described in the previous paragraph with the difference that the active parts of the sources are different. The density of the  $^{192}\text{Ir}$  active core was considered as  $22.42\text{ g/cm}^3$ .

In order to simulate the hypothetical  $^{57}\text{Co}$  source, the three most probable  $\gamma$  photons in the spectrum emitted by the radioisotope with energies of 136.47 keV (10.68%), 122.06 keV (85.6%) and 14.41 keV (9.16%) were defined (Table 1). Based on this spectrum, the average energy of photons emitted by  $^{57}\text{Co}$  is 114.17 keV. The spectrum of the  $^{192}\text{Ir}$  photons was considered based on the study by Medich *et al.* [12] (Table 2).

In order to verify the Flexisource  $^{192}\text{Ir}$  simulations, the dose rate constant and radial dose function for the  $^{192}\text{Ir}$  source were calculated and compared with those reported by Granero *et al.* on this source model [11].

#### TG-43 dosimetric parameters calculation

Dosimetric parameters introduced by TG-43U1 formalism [13] were calculated for the  $^{57}\text{Co}$  source. For this purpose, after source simulations, air kerma strength, dose rate constant, radial dose function and anisotropy function of the  $^{57}\text{Co}$  source were calculated. In order to have an accurate comparison of the  $^{57}\text{Co}$  and  $^{192}\text{Ir}$  sources, the obtained data were reported as tables and figures for both

Table 1. Photon energy spectrum of the hypothetical  $^{57}\text{Co}$  source used in this study

Energy (keV)	Prevalence (%)
136.47	10.68
122.06	85.6
14.41	9.16

Table 2. Photon energy spectrum of the  $^{192}\text{Ir}$  source used in this study [12]

Energy (keV)	Prevalence (%)
61.49	1.02
63.00	2.07
65.12	2.65
66.83	4.53
71.08	0.24
71.41	0.46
73.36	0.16
75.37	0.53
75.75	1.03
77.83	0.37
136.34	0.18
201.31	0.47
205.80	3.30
283.27	0.26
295.96	28.67
308.45	30.00
316.51	82.81
374.49	0.72
416.47	0.66
468.07	47.83
484.58	3.18
489.04	0.44
588.58	4.52
604.41	8.23
612.47	5.31
844.54	0.29
Total	230.12

sources. Finally, isodose curves around the  $^{57}\text{Co}$  and  $^{192}\text{Ir}$  sources were plotted in a single plot in order to compare the dose distributions of the sources. In the current study, MCNPX code (version 2.6.0) was utilized for all simulations [10]. The advantages of Monte Carlo simulation technique

in dosimetry in external beam radiation therapy and brachytherapy have been demonstrated for many years. Nowadays, the use of Monte Carlo simulation in radiotherapy applications is increasing because of the availability of high-speed computers and new Monte Carlo codes [14].

In order to calculate air kerma strength for the  $^{57}\text{Co}$  source, a number of 1 mm thick tori were defined at various radial distances ranging from 1 cm to 49 cm in free space, in the form of 50 cm radius spherical volume. Air was considered inside the tori. Electron and photon energy cut-offs were defined as equal to 250 eV, as adopted by Enger *et al.* [3]. The outputs were scored in the torus cells using F6 tally. The product of air kerma rate and the square of radial distance (air kerma rate  $\times d^2$ ) was plotted versus radial distance. The average value of this product in the relatively flat portion of the plot was used for calculation of air kerma strength. The calculation method of air kerma strength for the  $^{192}\text{Ir}$  source was the same as that of the  $^{57}\text{Co}$  source, except that the energy cut-off was set to 5 keV, because of its higher energy photons relative to  $^{57}\text{Co}$ . To calculate the air kerma strength for  $^{57}\text{Co}$ ,  $3 \times 10^8$  particles were run and the maximum type A MC statistical uncertainty was 0.2%. The calculation method for the  $^{192}\text{Ir}$  source is similar to  $^{57}\text{Co}$ , with the difference that the input file was run for  $4 \times 10^8$  particles and the maximum type A MC statistical uncertainty was 0.2% in calculation of air kerma strength.

For calculation of the dose rate constant, dose rate was calculated by means of a 0.1 cm thick torus at a distance of 1 cm from the source using \*F8 tally in a water phantom ( $\rho = 0.998 \text{ g/cm}^3$ ) with 50 cm radius. Energy cut-off was defined as the same as that for air kerma strength. Dry air up to the radius of 200 cm was defined outside of the spherical water phantom. The output of \*F8 tally was divided by the mass of the torus, then the dose rate constant was calculated by division of the dose rate value at 1 cm distance and air kerma strength. The input programs for  $^{57}\text{Co}$  and  $^{192}\text{Ir}$  sources were run for  $2 \times 10^8$  and  $3 \times 10^8$  particles, respectively, and the maximum type A MC statistical uncertainty was 0.1% in both calculations.

Radial dose functions were calculated at distances of 0.1–15 cm from the source in a water phantom with 50 cm radius. The thickness of the tori was 0.04 cm at distances lower than 1 cm, and after 1 cm the thickness was 0.1 cm. Outside the water sphere there was dry air up to a radius of 200 cm. The energy cut-off for particles in the case of  $^{57}\text{Co}$  was 250 eV. The outputs of \*F8 tally were divided by the masses of the tori. The energy cut-off for the  $^{192}\text{Ir}$  source was defined as 10 keV. A number of  $10^8$  particles were scored for  $^{57}\text{Co}$  and the maximum type A MC uncertainty was 1.77%. For the  $^{192}\text{Ir}$  source,  $8.5 \times 10^7$  particles were scored and the maximum uncertainty was 2.13% in the simulations.

In calculation of the anisotropy function for  $^{57}\text{Co}$  and  $^{192}\text{Ir}$  sources, 0.1 cm thickness tori were defined with 10-degree intervals at various distances ranging from 0.5 to 10 cm inside a 40 cm radius spherical water phantom. The energy cut-off for this calculation was similar to that in radial dose function calculation and the output was obtained by F6 tally. Anisotropy function values were ob-

tained using the outputs and geometric functions of the sources by use of linear source approximation. To calculate the anisotropy function, an active length of 3.5 mm was used for both  $^{57}\text{Co}$  and  $^{192}\text{Ir}$  sources in calculation of the geometric function with linear source approximation. A number of  $5 \times 10^7$  photons were scored for both sources and the maximum type A MC uncertainty for  $^{57}\text{Co}$  and  $^{192}\text{Ir}$  was 4.86% and 6.33%, respectively.

Finally, dosimetric parameters of the  $^{192}\text{Ir}$  source were compared with the corresponding published data. Dosimetric parameters of the  $^{57}\text{Co}$  source were compared with those of the  $^{192}\text{Ir}$  source.

### Isodose curves

In order to obtain the dose distribution around the  $^{57}\text{Co}$  and  $^{192}\text{Ir}$  sources, MCNPX code (version 2.6.0) was used. Type 1 mesh tally with the “pedep” option in Cartesian coordinates was utilized. The mesh cells were defined in the form of voxels with  $2 \times 2 \times 2 \text{ mm}^3$  dimensions, from -7 cm to +7 cm along the x- and y-axes. The input programs were run for  $2 \times 10^9$  particles, and the maximum type A MC statistical uncertainty was 0.3%. After running both programs, the output files, “mdata” files, were saved. These files are binary, and their contents are not directly accessible by a user. The outputs were converted to text files by means of “gridconv” command in MCNPX. The outputs were converted to matrices and the isodose curves were plotted using MATLAB software (version 7.8.0.347, Math Works Inc., Natick, MA). The output of type 1 mesh tally was in terms of  $\text{MeV/cm}^3$ , while the isodose curves were plotted in terms of  $\text{cGy} \cdot \text{h}^{-1} \cdot \text{U}^{-1}$ . In the first step of this conversion, the mesh tallies were divided by the density of the phantom and then were multiplied by other appropriate conversion factors to obtain the dose rate terms of  $\text{cGy} \cdot \text{h}^{-1} \cdot \text{U}^{-1}$ . Some of these conversion factors include unit conversion factors, source activities, source yields, etc. The yield values for  $^{192}\text{Ir}$  and  $^{57}\text{Co}$  radioisotopes are 2.3012 photons/disintegration and 1.0544 photons/disintegration, respectively. These values were calculated from the spectra data of these two sources in Tables 1 and 2.

### Results

Air kerma strength values per 1 mCi activity for the hypothetical  $^{57}\text{Co}$  source and Flexisource  $^{192}\text{Ir}$  source are  $0.46 \text{ cGy} \cdot \text{cm}^2 \cdot \text{h}^{-1} \cdot \text{mCi}^{-1}$  and  $3.62 \text{ cGy} \cdot \text{cm}^2 \cdot \text{h}^{-1} \cdot \text{mCi}^{-1}$ , respectively.

Dose rate constant values for the hypothetical  $^{57}\text{Co}$  and  $^{192}\text{Ir}$  sources are  $1.215 \text{ cGy} \cdot \text{h}^{-1} \cdot \text{U}^{-1}$  and  $1.114 \text{ cGy} \cdot \text{h}^{-1} \cdot \text{U}^{-1}$ , respectively. This quantity for the Flexisource  $^{192}\text{Ir}$  source reported by Granero *et al.* [11] is  $1.109 \text{ cGy} \cdot \text{h}^{-1} \cdot \text{U}^{-1}$ , which is 0.46% lower than the result presented above.

Radial dose function values from the current study and those reported by Granero *et al.* [11] for the Flexisource  $^{192}\text{Ir}$  source are presented in Table 3. Based on a comparison of these two data sets, it is evident that the Flexisource  $^{192}\text{Ir}$  simulation in this study is validated. The blank cells in this table represent those points which have no value reported by Granero *et al.* [11]; therefore, no comparison of these data points was performed. The maximum difference between these two data sets was 4.26%.

Radial dose function values for the hypothetical  $^{57}\text{Co}$  source are presented in Table 4. In order to compare radial dose function values of the two sources, radial dose function diagrams are presented in a single figure (Fig. 2).

Anisotropy function data for the hypothetical  $^{57}\text{Co}$  and  $^{192}\text{Ir}$  sources are listed in Tables 5 and 6, respectively. To compare anisotropy function values of these sources, the corresponding diagrams are plotted in Fig. 3 for four distances of 0.5, 1, 5 and 10 cm.

A comparison of isodose curves for these two sources may be interesting. Isodose curves of the two sources are plotted in Fig. 4. The dose rate values in these figures were obtained using mesh tallies in MCNPX code and were plotted in the MATLAB software environment.

## Discussion

In the current study, TG-43 dosimetric parameters and dose distributions for a hypothetical  $^{57}\text{Co}$  source and Flexisource  $^{192}\text{Ir}$  source were calculated and reported. The geometries of the  $^{57}\text{Co}$  and  $^{192}\text{Ir}$  sources were the same, except for the compositions of the active parts of the sources. Some criteria which should be considered in radiation therapy are appropriate accuracy in dose calculations, dose delivery and adequate dose distribution relative to the expected situation. Air kerma strength per mCi activity for the hypothetical  $^{57}\text{Co}$  source is less than that of the  $^{192}\text{Ir}$  source ( $0.46 \text{ cGy}\cdot\text{cm}^2\cdot\text{h}^{-1}\cdot\text{mCi}^{-1}$  for  $^{57}\text{Co}$  and  $3.62 \text{ cGy}\cdot\text{cm}^2\cdot\text{h}^{-1}\cdot\text{mCi}^{-1}$  for  $^{192}\text{Ir}$ ). This effect is due to the difference in the photon yields and photon energy spectra emitted by these two sources. The average photon energy for  $^{57}\text{Co}$  and  $^{192}\text{Ir}$  is 114.17 keV and 360 keV, respectively. From the air kerma strength data of the two sources it can be concluded that in the same conditions, air kerma strength for  $^{192}\text{Ir}$  is greater than that of  $^{57}\text{Co}$ , which is considered an advantage for the  $^{192}\text{Ir}$  source over  $^{57}\text{Co}$ . However, if both sources have the same initial activities, due to the lower half-life of  $^{192}\text{Ir}$ , its air kerma strength will decrease at a faster rate. With the same initial activities, after about four half-lives of  $^{192}\text{Ir}$ , the air kerma strength of  $^{57}\text{Co}$  will be equal to that of the  $^{192}\text{Ir}$  source, which can be considered as an advantage of the  $^{57}\text{Co}$  source. By comparison between the dose rate constant values ( $1.215 \text{ cGy}\cdot\text{h}^{-1}\cdot\text{U}^{-1}$  and  $1.114 \text{ cGy}\cdot\text{h}^{-1}\cdot\text{U}^{-1}$  for  $^{57}\text{Co}$  and  $^{192}\text{Ir}$ , respectively) it can be seen that per U of air kerma strength,  $^{57}\text{Co}$  can produce a higher dose rate at the reference distance (1 cm) from the source in water medium.

In order to compare the radial dose function values of the two sources (Fig. 2), the photon interactions in phantom material should be interpreted. The energies of the emitted photons from the brachytherapy sources affect photon absorption in the phantom. For relatively high energy brachytherapy sources such as  $^{192}\text{Ir}$ , the total dose distribution is not mainly from the scattered photons in the typical brachytherapy range. However, the photon absorption in the phantom material is compensated by scattering of low energy photons. As can be seen from the data in Fig. 2, the radial dose function for the  $^{192}\text{Ir}$  source is more uniform due to build up of the scattering component of

**Table 3.** Radial dose function for the Flexisource  $^{192}\text{Ir}$  source obtained in this study in comparison to the data of Granero *et al.* [11]

Radial distance $r$ (cm)	(Our study)	Granero <i>et al.</i>	Diff. (%)
0.1	1.0715	–	–
0.2	1.0050	–	–
0.3	1.0002	–	–
0.4	1.0169	–	–
0.5	1.0058	0.9983	0.75
1.0	1.0000	1.0000	0.00
1.5	1.0242	1.0017	2.24
2.0	1.0225	1.0037	1.87
2.5	1.0285	–	–
3.0	1.0143	1.0051	0.92
3.5	1.0373	–	–
4.0	1.0268	1.0034	2.33
4.5	1.0203	–	–
5.0	1.0199	0.9987	2.12
7.5	1.0092	–	–
10.0	0.9662	0.9349	3.35
12.0	0.9317	0.8937	4.26
15.0	0.8308	0.8212	1.17

**Table 4.** Radial dose function for the hypothetical  $^{57}\text{Co}$  source obtained in this study

Radial distance $r$ (cm)	$g_r(r)$
0.1	0.917
0.2	0.916
0.3	0.923
0.4	0.946
0.5	0.950
1.0	1.000
1.5	1.043
2.0	1.080
2.5	1.126
3.0	1.176
3.5	1.219
4.0	1.210
4.5	1.244
5.0	1.277
7.5	1.322
10.0	1.305
12.0	1.286
15.0	1.125

the dose. For sources with medium energy, such as  $^{57}\text{Co}$ , dose distribution is mainly influenced by multiple scattered low energy photons. Therefore, as shown in Fig. 2, this source has an increase in radial dose function which is specific for this energy range. From this point of view,

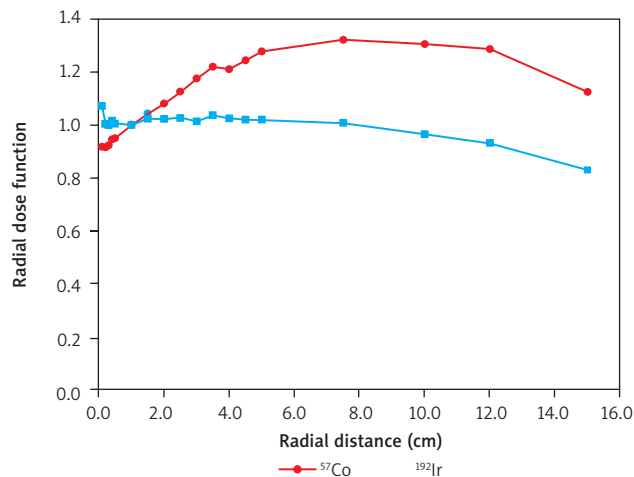


**Fig. 2.** Radial dose function for the hypothetical  $^{57}\text{Co}$  and  $^{192}\text{Ir}$  sources obtained in this study versus radial distance from the source

the  $^{192}\text{Ir}$  source has a more uniform dose distribution at various radial distances from the source, compared to the  $^{57}\text{Co}$  source. The same effect for the radial dose function of these two sources was reported by Enger *et al.* [3].

In the study by Enger *et al.* [3] the anisotropy function was reported only at a distance of 1 cm from the hypothetical  $^{57}\text{Co}$  source in the form of a diagram. In the current study, in addition to the diagram presentation of the anisotropy function for various distances (Fig. 3), the tabulated data for various distances are also presented for this

source (Table 5). Due to the lack of any tabulated data, it is not possible to make a comparison between the data from this study and other studies for the hypothetical  $^{57}\text{Co}$  source. The anisotropy function diagram by Enger *et al.* [3] contains some fluctuations. The shape of the tally cells used in calculation of the anisotropy function was not described in the materials and methods section of that study. It can be guessed that spherical or cubic cells were used. This may be the origin of fluctuations in anisotropy function values of the source. In this study, tori were used in order to preserve the cylindrical symmetry. As demonstrated in Fig. 3, there is no fluctuation in anisotropy function data in the current study. At all distances and various angles, anisotropy function data for  $^{57}\text{Co}$  are closer to 1.00 relative to the data for  $^{192}\text{Ir}$ . This effect may be considered as an advantage of  $^{57}\text{Co}$  versus the  $^{192}\text{Ir}$  source.

Isodose curves for the  $^{57}\text{Co}$  and  $^{192}\text{Ir}$  sources are plotted in Fig. 4. When one considers these curves, isodose curves of  $^{57}\text{Co}$  for the same dose contour values are located outside the corresponding contours of the  $^{192}\text{Ir}$  source, except for the 300  $\text{cGyh}^{-1}\text{U}^{-1}$  contour. This effect implies that at the same points, the dose rate of  $^{57}\text{Co}$  is higher than  $^{192}\text{Ir}$ . From Fig. 2, the same results are expected for the radial dose function. Also, except for distances less than 1 cm, the radial dose function curve of  $^{57}\text{Co}$  is greater than that of  $^{192}\text{Ir}$ . This is another advantage of the  $^{57}\text{Co}$  source. In Fig. 4, the cable of the source is located at the left side of the plot. At the left end of the sources, in the position of the cables, the magnitude of the dose contour dip for  $^{57}\text{Co}$  and  $^{192}\text{Ir}$  in the isodose curves are the same. However,

**Table 5.** Anisotropy function data for the hypothetical  $^{57}\text{Co}$  source obtained in this study

$\theta(^{\circ})$	Distance $r$ (cm)							
	0.5	1	2	3	4	5	7.5	10
0	0.779	0.774	0.786	0.814	0.846	0.886	0.845	0.956
10	0.812	0.824	0.855	0.877	0.894	0.907	0.928	0.950
20	0.900	0.905	0.917	0.925	0.940	0.943	0.953	0.964
30	0.944	0.947	0.952	0.958	0.961	0.966	0.972	0.985
40	0.972	0.969	0.973	0.975	0.976	0.978	0.983	0.989
50	0.984	0.981	0.986	0.988	0.988	0.987	0.990	0.993
60	0.992	0.992	0.994	0.994	0.995	0.995	0.997	1.000
70	0.996	0.996	0.997	0.997	0.995	0.995	0.996	1.009
80	1.000	0.999	0.999	1.000	1.001	0.999	1.001	1.003
90	1.000	1.000	1.000	1.000	1.000	1.000	1.000	1.000
100	0.999	0.997	0.998	1.000	0.999	1.000	0.997	1.005
110	0.996	0.995	0.998	0.997	1.000	0.997	0.995	1.004
120	0.993	0.992	0.992	0.992	0.993	0.992	0.992	1.000
130	0.985	0.985	0.987	0.988	0.989	0.988	0.995	0.998
140	0.971	0.972	0.975	0.976	0.980	0.981	0.985	0.986
150	0.949	0.950	0.957	0.966	0.967	0.968	0.972	0.982
160	0.910	0.911	0.923	0.934	0.940	0.946	0.956	0.971
170	0.822	0.823	0.850	0.871	0.891	0.903	0.919	0.937
180	–	0.454	0.578	0.642	0.715	0.759	0.850	0.913

**Table 6.** Anisotropy function data for the Flexisource <sup>192</sup>Ir source obtained in this study

$\theta(^{\circ})$	Distance $r$ (cm)							
	0.5	1	2	3	4	5	7.5	10
0	0.671	0.638	0.640	0.649	0.679	0.700	0.747	0.752
10	0.735	0.729	0.745	0.763	0.779	0.791	0.818	0.839
20	0.850	0.846	0.852	0.860	0.868	0.875	0.890	0.892
30	0.913	0.912	0.912	0.916	0.920	0.923	0.932	0.940
40	0.951	0.947	0.948	0.950	0.952	0.954	0.956	0.958
50	0.972	0.968	0.971	0.970	0.971	0.971	0.974	0.977
60	0.985	0.985	0.987	0.989	0.991	0.991	0.992	0.993
70	0.993	0.994	0.993	0.993	0.995	0.993	0.994	1.003
80	0.998	0.999	0.999	0.998	1.000	0.999	1.000	1.002
90	1.000	1.000	1.000	1.000	1.000	1.000	1.000	1.000
100	0.998	0.997	0.997	0.998	0.999	0.999	1.001	1.001
110	0.993	0.994	0.996	0.995	0.995	0.993	0.995	1.002
120	0.987	0.985	0.985	0.986	0.987	0.987	0.989	0.991
130	0.973	0.971	0.973	0.973	0.973	0.971	0.976	0.977
140	0.952	0.950	0.949	0.950	0.950	0.954	0.960	0.962
150	0.916	0.912	0.915	0.920	0.926	0.928	0.933	0.938
160	0.856	0.848	0.855	0.862	0.868	0.876	0.897	0.912
170	0.738	0.728	0.746	0.758	0.778	0.791	0.823	0.842
180	–	0.498	0.528	0.554	0.588	0.625	0.680	0.785

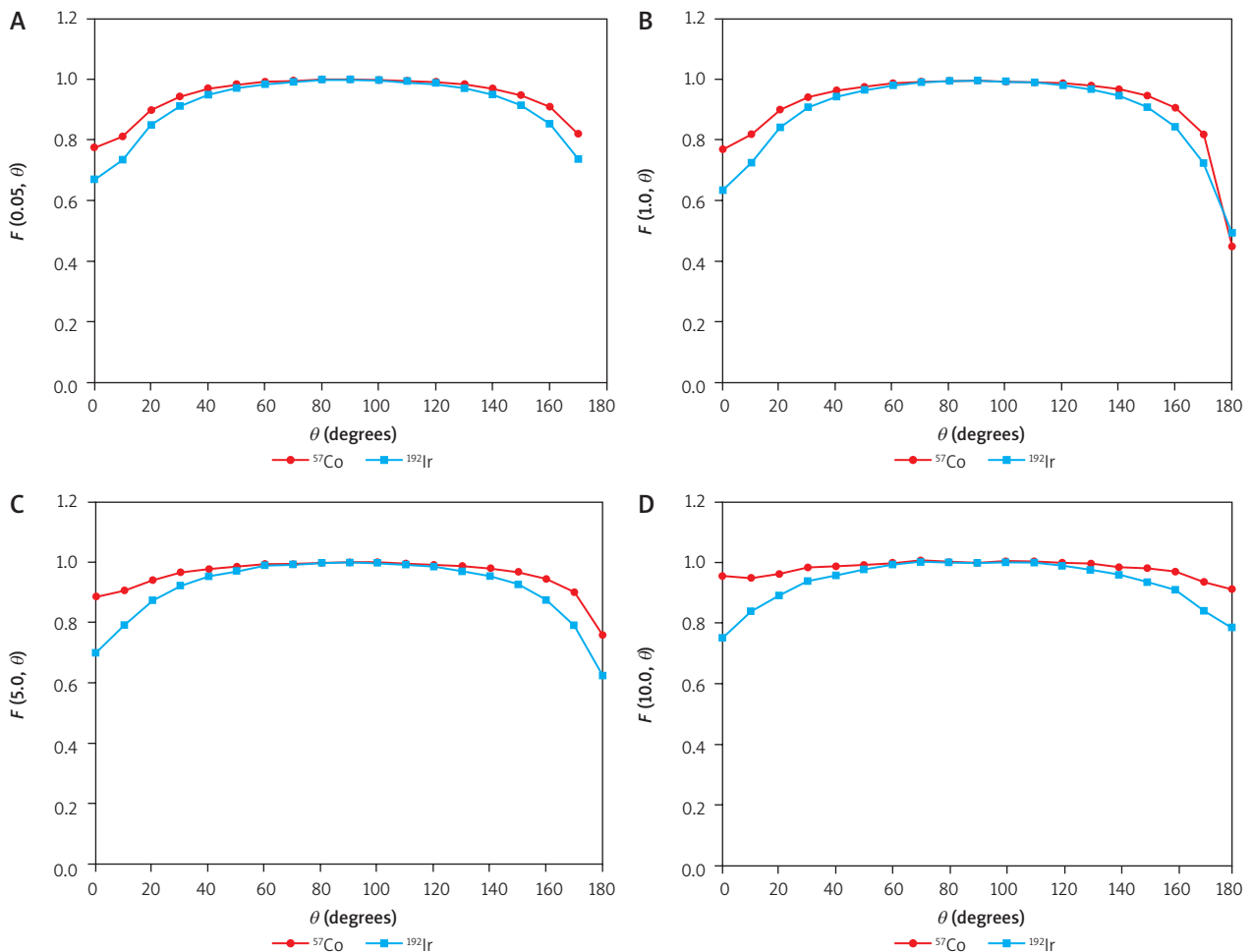


**Fig. 3.** Anisotropy function for the hypothetical <sup>57</sup>Co and <sup>192</sup>Ir sources obtained in this study versus the angle for distances of: A) 0.5 cm, B) 1 cm, C) 5 cm, D) 10 cm from the source

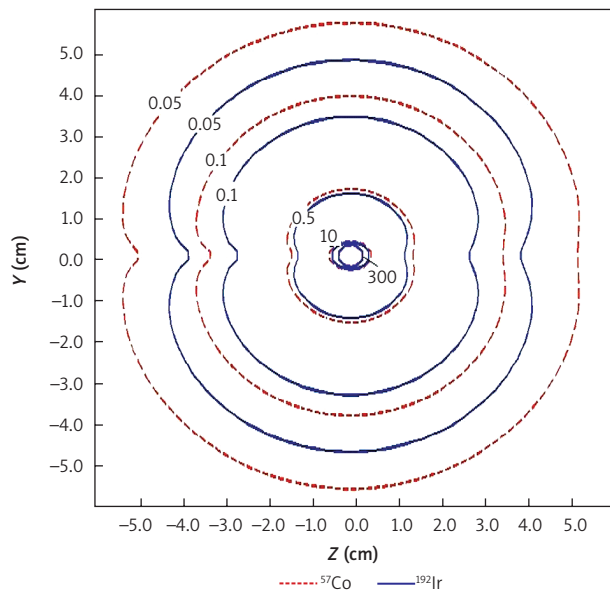


**Fig. 4.** Isodose curves for the  $^{57}\text{Co}$  hypothetical and  $^{192}\text{Ir}$  sources in terms of  $\text{cGy}\cdot\text{h}^{-1}\cdot\text{U}^{-1}$  in the longitudinal plane ( $y$ - $z$  plane). The  $z$  coordinate is coincident with the longitudinal axis of the source

at the right end of the sources, in the position of the tip of the sources, the amount of dip in the contours of the  $^{57}\text{Co}$  isodose curves are somewhat less than for  $^{192}\text{Ir}$ . This provides a more uniform dose distribution for the  $^{57}\text{Co}$  source. The same results are evident from the anisotropy function comparisons of  $^{57}\text{Co}$  and  $^{192}\text{Ir}$  sources in Fig. 3.

In conclusions the hypothetical  $^{57}\text{Co}$  source were to be made available commercially, with the same geometry as designed in this study, the data presented herein could be used as input data for a treatment planning system and also in verification of the system calculations after commissioning of the unit including this radioisotope.

The beneficial characteristics of the  $^{57}\text{Co}$  radioisotope make it a possible future brachytherapy source. This source has a combination of possible high specific activity (312  $\text{TBq/g}$  [15]), relatively medium energy photon emission and an appropriate half-life (272 days).  $^{57}\text{Co}$  decays by electron capture, and it is converted to  $^{57}\text{Fe}$  by gamma emission. The half-life of  $^{57}\text{Co}$  is about four times longer than that of the  $^{192}\text{Ir}$  source (74 days). Therefore, due to the longer half-life of the  $^{57}\text{Co}$  radioisotope in comparison to other available brachytherapy sources, it needs fewer source calibrations and exchanges, which may reduce costs. Half-value layers for  $^{57}\text{Co}$  and  $^{192}\text{Ir}$  are 0.145 mm and 2.5 mm, respectively. Therefore, lower shielding thickness is needed around a  $^{57}\text{Co}$  source compared to  $^{192}\text{Ir}$ . The higher dose rate constant and more isotropic anisotropy functions and more uniform dose distributions relative to  $^{192}\text{Ir}$  are other advantages of the  $^{57}\text{Co}$  source relative to  $^{192}\text{Ir}$ . However, the initial air kerma strength for  $^{192}\text{Ir}$  is higher than that of  $^{57}\text{Co}$ , and the radial dose function of  $^{192}\text{Ir}$  is more uniform than that of  $^{57}\text{Co}$ . The two latter points can be considered as advantages of  $^{192}\text{Ir}$  over  $^{57}\text{Co}$ .

The authors would like to thank the Iran National Science Foundation (INSF) for financial support of this work. The authors declare no conflict of interest.

#### References

1. Cai W, Gao T, Hong H, Sun J. Applications of gold nanoparticles in cancer nanotechnology. *Nanotechnol Sci Appl* 2008; 1: 17-32.
2. Awan SB, Dini SA, Hussain M, Meigooni DS, Meigooni AS. Cylindrical coordinate based TG-43U1 parameters for dose calculation around elongated brachytherapy sources. *J Appl Clin Med Phys* 2008; 9: 123-42.
3. Enger SA, Lundqvist H, D'Amours M, Beaulieu L. Exploring  $^{57}\text{Co}$  as a new isotope for brachytherapy applications. *Med Phys* 2012; 39: 2342-5.
4. Carter AJ, Laird JR. Experimental results with endovascular irradiation via a radioactive stent. *Int J Radiat Oncol Biol Phys* 1996; 36: 797-803.
5. Ballester F, Granero D, Perez-Calatayud J, Venselaar JL, Rivard MJ. Study of encapsulated  $^{170}\text{Tm}$  sources for their potential use in brachytherapy. *Med Phys* 2010; 37: 1629-37.
6. Enger SA, D'Amours M, Beaulieu L. Modeling a hypothetical  $^{170}\text{Tm}$  source for brachytherapy applications. *Med Phys* 2011; 38: 5307-10.
7. Enger SA, Fisher DR, Flynn RT. Gadolinium-153 as a brachytherapy isotope. *Phys Med Biol* 2013; 58: 957-64.
8. Mason DL, Battista JJ, Barnett RB, Porter AT. Ytterbium-169: Calculated physical properties of a new radiation source for brachytherapy. *Med Phys* 1992; 19: 695-703.
9. Ninkovic MM, Raicevic JJ, Adrovic F. Air kerma rate constants for gamma emitters used most often in practice. *Radiat Prot Dosimetry* 2005; 115: 247-50.
10. Pelowitz D. MCNPX users manual, LA-CP-07-1473 Version 2.6.0, 2008, Los Alamos National Laboratory.
11. Granero D, Pérez-Calatayud J, Casal E, Ballester F, Venselaar J. A dosimetric study on the Ir-192 high dose rate Flexisource. *Med Phys* 2006; 33: 4578-82.
12. Medich DC, Munro JJ 3rd. Monte Carlo characterization of the M-19 high dose rate Iridium-192 brachytherapy source. *Med Phys* 2007; 34: 1999-2006.
13. Rivard MJ, Coursey BM, DeWerd LA, et al. Update of AAPM Task Group No. 43 Report: A revised AAPM protocol for brachytherapy dose calculations. *Med Phys* 2004; 31: 633-74.
14. Zhang H, Baker C, McKinsey R, Meigooni A. Dose verification with Monte Carlo technique for prostate brachytherapy implants with  $^{125}\text{I}$  sources. *Med Dosim* 2005; 30: 85-91.
15. Enger SA, Beaulieu L. Modeling a hypothetical  $^{57}\text{Co}$  source for brachytherapy application. *Brachytherapy* 2011; 10 (Suppl 1): S33.

#### Address for correspondence

**Mahdi Ghorbani**, PhD  
 Medical Physics Department, Faculty of Medicine  
 Mashhad University of Medical Sciences  
 Paradise Daneshgah, Vakil Abad Blvd., Mashhad, Iran  
 Postal zip code: 9177948564  
 e-mail: mhdghorbani@gmail.com  
 tel. +98 51 38002316  
 fax +98 51 38002320

**Submitted:** 6.04.2015

**Accepted:** 30.11.2015